RSC Advances

PAPER

View Article Online
View Journal | View Issue

Cite this: *RSC Adv.*, 2017, **7**, 1443

Catalytic activity of transition metal doped Cu(111) surfaces for ethanol synthesis from acetic acid hydrogenation: a DFT study

Minhua Zhang,[ab] Rui Yao,[ab] Haoxi Jiang,*[ab] Guiming Li[ab] and Yifei Chen[ab]

Transition metal (Co, Ni, Ru, Rh, Pd and Pt) doped Cu(111) models are selected to examine the effects of transition metals on Cu surface for ethanol synthesis from acetic acid hydrogenation using density functional theory (DFT) calculations. On these surfaces, the adsorption of the main intermediates and reaction barriers of key elementary steps are investigated. The calculation results indicate that oxophilic metals are projected to be more active in acetic acid adsorption and acetaldehyde adsorption compared to less-oxophilic metals. Those metals with larger C adsorption energies generally have better C–OH bond cracking activity. Additionally, a good linear Brønsted–Evans–Polanyi (BEP) correlation is established for predicting the preferences of C–OH bond scission of acetic acid on other metals. Finally, O–H bond formation in C_2-oxygenates (CH_3CO, CH_3CHO, CH_3CH_2O) hydrogenation is examined on all these surfaces. The reactions are more likely to occur on less-oxophilic metal-doped Cu surfaces. Therefore, it appears to involve an intricate balance between C–OH cracking and O–H bond formation reactions. That means those metal-doped Cu-based catalysts that are capable of preferentially activating C–OH bond without considerably inhibiting O–H bond formation of C_2-oxygenates are predicted to achieve optimum catalytic activity for ethanol synthesis from acetic acid hydrogenation. The results can provide theoretical guidance for related experiments as well as the designing of Cu-based catalysts for ethanol synthesis.

Received 6th November 2016
Accepted 16th December 2016

DOI: 10.1039/c6ra26373a

www.rsc.org/advances

1. Introduction

Acetic acid, as one of the main short chain fatty acids, can be produced by anaerobic fermentation or pyrolysis of biomass.[1] At the same time, the syngas route has also become an alternative route for acetic acid production. In recent years, the overcapacity in the acetic acid industry has brought about sustained decreases in the acetic acid price.[2,3] Therefore, it is imperative to purposely synthesize more valuable chemicals using acetic acid as a raw material. The hydrogenation of acetic acid ($CH_3COOH + 2H_2 \rightarrow CH_3CH_2OH + H_2O$) is an alternative route for ethanol production and has not been systematically investigated hitherto. Ethanol has been regarded as a potential carbon-neutral fuel source over the past decades and also can be used for producing many value-added chemicals.[4,5] In addition, ethanol has received wide attentions as a substitute for a series of biomass-derived molecules.[6] Above all, it is rather meaningful of transferring acetic acid to ethanol through consecutive hydrogenation reactions from an economical and feasible point of view.

Currently, the catalysts applied in the process of acetic acid hydrogenation to ethanol are mainly noble metals, including Pt, Pd and Ru, alloyed with a second metal (such as Co, Ni and Cu) as promoter. These noble metal-based catalysts have been proved to show excellent catalytic performance and some have realized industrialization in many countries in recent years. However, the underlying reaction mechanism of the hydrogenation of acetic acid to ethanol has not been investigated profoundly. Only a few researchers have focused on this issue recently. Rachmady *et al.*[7] applied Pt/TiO_2 catalyst for acetic acid hydrogenation to ethanol and acquired a selectivity of 70%. They proposed that the reaction take place *via* adsorbed hydrogen atoms on metal and acetyl groups on TiO_2 support rather than acetic acid or acetate groups and the product ethanol mainly forms from acetaldehyde. Alcala *et al.*[8] compared acetic acid conversion over silica-supported Pt and Pt–Sn catalysts. Their results presented that the addition of Sn can help inhibit C–O bond and C–C bond cleavage in oxygenated hydrocarbons. Compared with the main products CO, CH_4 and C_2H_6 over Pt catalyst, the products on Pt–Sn catalyst are mainly ethanol, acetaldehyde and ethyl acetate. Pallassana and co-workers[9] postulated the most preferable pathway of acetic acid hydrogenolysis to ethanol on Pd catalyst involves acetic acid dissociation to acetyl, followed by successive hydrogenation to acetaldehyde and ethanol. They suggested that the rate-

[a]*Key Laboratory for Green Chemical Technology of Ministry of Education, R&D Center for Petrochemical Technology, Tianjin University, Tianjin 300072, PR China. E-mail: hxjiang@tju.edu.cn; Fax: +86-22-27406119; Tel: +86-22-27406119*

[b]*Collaborative Innovation Center of Chemical Science and Engineering (Tianjin), Tianjin 300072, PR China*

determining step is C–OH bond activation. For Ru catalyst, Olcay and co-workers[10,11] concluded that the high activity is attributed to its strong ability of activating the initial scission of C–OH bond.

Although the noble metal-based catalysts show nice catalytic performance, applications of such noble metal catalysts in industry might be greatly restricted because of their high price and limited resources. Therefore, it is not only economically-valuable, but also resource-saving, if we can exploit a cheaper and more active catalytic system for acetic acid hydrogenation compared to noble metals.

Copper, one of the non-noble metals, has been widely used in many hydrogenation reactions[12–19] as an effective catalyst, such as CO or CO_2 hydrogenation to methanol or ethanol, acetyl acetate hydrogenation to ethanol, and 2-furfuraldehyde hydrogenation. This means Cu-based catalysts have great potentials to be applied in the process of acetic acid hydrogenation. More importantly, it would significantly reduce the cost if the effective Cu-based catalysts are developed for ethanol synthesis from acetic acid. Onyestyák *et al.*[20–22] investigated the performance of Cu-based for acetic acid hydrogenation, and their experiment results[23–25] indicated that the main products are ethanol, acetyl acetate, acetaldehyde and water on pure Cu catalyst. However, the yield of ethanol is relatively low and it can be improved through doping oxide In_2O_3 due to the alloy phase Cu_2In formation.

Although Cu catalyst has been proved to be an effective catalyst in hydrogenation processes, some researchers[6,17,26] still believe that C–O bond and C–C bond scission of oxygenates might not occur easily on Cu surface compared to other noble metals. Dumesic *et al.*[26] believed that compared with ethyl acetate dissociation to acetyl and acetate, acetic acid is more difficult to dissociate on Cu catalyst, which leads to lower ethanol yield with the main products ethanol, acetaldehyde and ethyl acetate. Olcay and co-workers[10] also suggested that acetic acid conversion must involve C–OH bond scission followed by hydrogenation reactions, and the initial C–OH bond cleavage is the rate-determined step. Therefore, acetic acid dissociation to acetyl and hydroxyl is the indispensable descriptor for acetic acid conversion. This elementary step ($CH_3COOH \rightarrow CH_3CO + OH$) is chosen as one of main concerns for screening alloyed Cu catalysts.

In addition, O–H bond formation for C_1-oxygenates and C_2-oxygenates was reported to be more difficult than C–H bond formation on Cu catalyst.[14,15,17] However, O–H bond formation is an unavoidable step for acetic acid hydrogenation. Therefore, O–H bond formation is considered as another descriptor which could have considerable effects on the selectivity and yield of ethanol.

Alloying second noble metal is a promising way to promote the performance of non-noble metal catalysts.[27–41] Various noble metals (Au, Pd, Rh, Pt, Ni) were doped on Cu(111) in the hydrogenation of CO_2 to methanol, and Ni/Cu(111) was reported to have the highest methanol yield, followed by Pt, Rh, Pd and Au.[18] Spivey *et al.*[27] suggested the ethanol yield can be greatly enhanced on bimetallic catalysts because of synergistic effect. Zhao and co-workers[35] reported that Rh-decorated Cu alloys show the lowest reaction barriers of CO insertion and the noticeable increase of the selectivity of C_2-oxygenates through DFT calculations.

At present, there are few theoretical and experimental evidences about which metal can enhance the performance of Cu catalyst for acetic acid hydrogenation. So our work mainly focus on the effects of transition metal dopants into Cu surface for acetic acid hydrogenation to ethanol, which is conductive for us to screen potential Cu-based catalysts with excellent catalytic performance. So in this paper, we determined the mechanism of acetic acid hydrogenation to ethanol on the Cu(111) surface doped by other transition metals (Co, Ni, Ru, Rh, Pd and Pt) using DFT calculations. According to the descriptors mentioned above, this work is aimed to provide insights into the effects of doped-metals on the intermediates and transition states of key elementary steps.

2. Computational methods

All our DFT calculations of adsorption energies and reaction barriers were performed using Dmol^3 module in Material Studio Package with the generalized gradient approximation (GGA) for the exchange and correlation functional in the form of Perdew–Burke–Ernzerhof (PBE).[42,43] DFT semi-core pseudopotential (DSPP) was set for the core treatment to balance calculation accuracy and computational efficiency and the basic set was expanded in terms of a double numerical plus polarization (DNP). The surface Brillouin zone was sampled by a $3 \times 3 \times 1$ *k*-point mesh according to Monkhorst–Pack method and a Methfessel–Paxton smearing of 0.005 Ha was conducted to accelerate convergence. The convergence criteria included threshold values of 2×10^{-5} Ha for energy, 0.004 Ha Å^{-1} for maximum force, and 0.005 Å for maximum displacement, with the self-consistent-field (SCF) density convergence threshold value of 1×10^{-5} Ha. Spin polarization was also involved in our calculations for all metal surfaces.

The Cu(111) surface was modelled using a three-layer slab with a (4×4) unit cell and only the top layer was allowed to relax while the two bottom layers were fixed in the optimized bulk position as literatures.[18,26] A 15 Å of vacuum space between the periodic slabs was utilized to eliminate spurious interactions. Three Cu atoms on the Cu(111) surface were substituted by other transition metals in each unit cell as alloy models, which means the corresponding coverage is 3/16 ML. It has been proved that among all the dopants, Pd, Pt favor to stay in the Cu surface, while Ni, Co, Ru and Rh prefer the bulk.[44] However, we believe that the effect of the experimental environment should also be considered. According to the calculations from Fu,[45] they concluded that under the hydrogen-rich environments, most of the alloyed metal atoms (except Fe), can stably occupy the surface layer. And also, according to the study by Greeley *et al.*,[46] adsorbed hydrogen on the surface can draw the metal atom to the surface layer of the alloy system under the actual conditions of hydrogenation. Similarly, according to the experiments by Chorkendorff *et al.*[47] for CO hydrogenation to CH_3OH, Ni atoms can be pulled out to the surface by the active adsorbates such as CO. Therefore, the

surface segregation between doped transition metals and Cu was not included in our present study.

The transition state (TS) searches of elementary reactions were carried out at the same theoretical level as those for the optimization of reactants and products with complete linear synchronous transit/quadratic synchronous transit (LST/QST) method.[48,49] Each TS structure was confirmed by the vibrational analysis with only one imaginary frequency along the reaction coordinate. Zero-point energy corrections (ZPE) were considered with harmonic oscillator approach based on the calculations of vibrational frequencies.

The adsorption energies of all species on metal surfaces were calculated according to the following formula:

$$E_{ads} = E_{Cu/M} + E_{adsorbates} - E_{adsorbates\text{-}Cu/M}$$

where $E_{Cu/M}$, $E_{adsorbates}$ and $E_{adsorbates\text{-}Cu/M}$ were the total energies of Cu/M substrate, the free adsorbate and the adsorbate-Cu/M substrate, respectively.

The activation barriers and reaction energies are defined as:

$$E_a = E(TS) - E(IS)$$

$$\Delta E = E(FS) - E(IS)$$

where E(IS), E(TS), E(FS) represents the total energies of the initial states, transition states and final states, respectively. Positive value of ΔE refers to endothermic reaction.

3. Results and discussion

In the present study, DFT calculations were performed to study the transition states (TS) and intermediates of acetic acid hydrogenation to ethanol on pure Cu and Cu–metal alloys for the first time. In order to figure out proper transition metals which can have positive effects on Cu catalysts, six kinds of transition metals (Co, Ni, Ru, Rh, Pd and Pt) are doped into Cu(111) surface as representative models. The two descriptors mentioned above on different metal-doped Cu surfaces are calculated and discussed in detail in the following sections, and those on pure Cu surface are also examined for comparison.

3.1 Acetic acid scission

3.1.1 CH_3COOH adsorption. The most stable adsorption configurations and adsorption energies of CH_3COOH on pure Cu and six metal-doped Cu surfaces are summarized in Fig. 1 and Table 1. It can be seen from Table 1 that acetic acid is easy to desorb from Cu surface rather than undergo further reactions because of the weak adsorption energy (0.30 eV). We expect that the doping of second metal could strengthen the adsorption of acetic acid molecules and favor subsequent reactions.

We can see from Fig. 1 that CH_3COOH prefer to adsorb on Cu(111), CuCo(111), CuNi(111), CuRu(111), CuRh(111) and CuPd(111) surfaces with one O(C═O) residing on top of a Cu or doped-metal atom, while on CuPt(111) surface, O atom (C═O) is more likely to adsorb at the top of Cu atom which is adjacent to a Pt atom. The adsorption energies of acetic acid on Co, Ni, Ru, Rh, Pd and Pt doped Cu(111) are 0.84, 0.47, 0.75, 0.46, 0.32 and 0.37 eV, respectively. Compared with that on Cu(111) surface, additions of Co and Ru are able to significantly increase acetic acid adsorption energy. Meanwhile, Ni and Rh can also enhance the adsorption energy to a certain extent. However, doping Pt and Pd into Cu(111) is proved to be not effective to enhance the adsorption. Above result means more acetic acid species can be adsorbed on CuCo and CuRu surfaces.

3.1.2 Reaction barrier of CH_3COOH scission

$CH_3COOH \rightarrow CH_3CO + OH$. CH_3CH_2OH synthesis from acetic acid and H_2 is limited by the higher reaction barrier of CH_3COOH dissociation and this reaction is the rate-determining step on Cu catalyst according to some studies mentioned above. In addition, the activation energy of acetic acid dissociation to acetyl on pure Cu surface is 1.53 eV though our calculations, which means this step is more difficult to occur on Cu under normal experimental conditions. Therefore, for the sake of improving the catalytic performance of Cu catalyst, the selected doped metals should have ability to reduce the reaction barrier of CH_3COOH scission directly and hence improve CH_3COOH conversion rate. Schematic representations of transition states (TSs) corresponding to the elementary reaction of $CH_3COOH \rightarrow CH_3CO + OH$ on each doped metal Cu(111) surface are also depicted in Fig. 1 and the reaction barriers and reaction energies on various metal-doped Cu surfaces are listed in Table 1. From Table 1, we can see that the reaction barriers for breaking C–OH bond of acetic acid on six different surfaces vary greatly. Co, Ni, Ru and Rh doped Cu surfaces, are considered to be more catalytically active than pure Cu(111), with reaction barriers 0.14, 0.55, 0.66, and 0.74 eV, while Pt only shows slight improvement for C–OH bond scission (1.23 eV). In addition, on CuCo(111), the reaction energy of this reaction is found to be the most exothermic, which is in consistent with its lowest reaction barrier among all metals. Interestingly, the adsorption energy of acetic acid on CuCo(111) surface is larger than its dissociation barrier, which means acetic acid is more likely to dissociate to acetyl and hydroxyl than to desorb from surface. However, on other metal-doped surfaces and pure Cu surface, acetic acid does not interact strongly enough with metal surfaces and tends to desorb from those into vapour phase.

3.1.3 Correlations between C–OH bond scission and atomic adsorption energies. Different metals play different roles in the stability of adsorbates, and thus we are devoted to understand the trends in adsorption energies of atoms and reaction barriers among metals. Sutton *et al.*[6] studied the adsorption and activation of ethanol on six transition metal surfaces (Co, Ni, Pd, Pt, Rh and Ru). The calculations results indicated that compared with others, those metal surfaces with stronger C adsorption are predicted to be more active, while metals with high O adsorption energies (especially relative to their C adsorption energies), are considered to be more selective to C–O scission of ethanol, whereas those with weaker O adsorption should be more selective to C–C scission. Gomes and co-workers[50] also believed that binding energy of the O atom is still a qualitative descriptor for O–H bond scission in methanol. Therefore, in order to acquire more insights into C–OH bond scission of acetic acid, we calculate C and O atoms

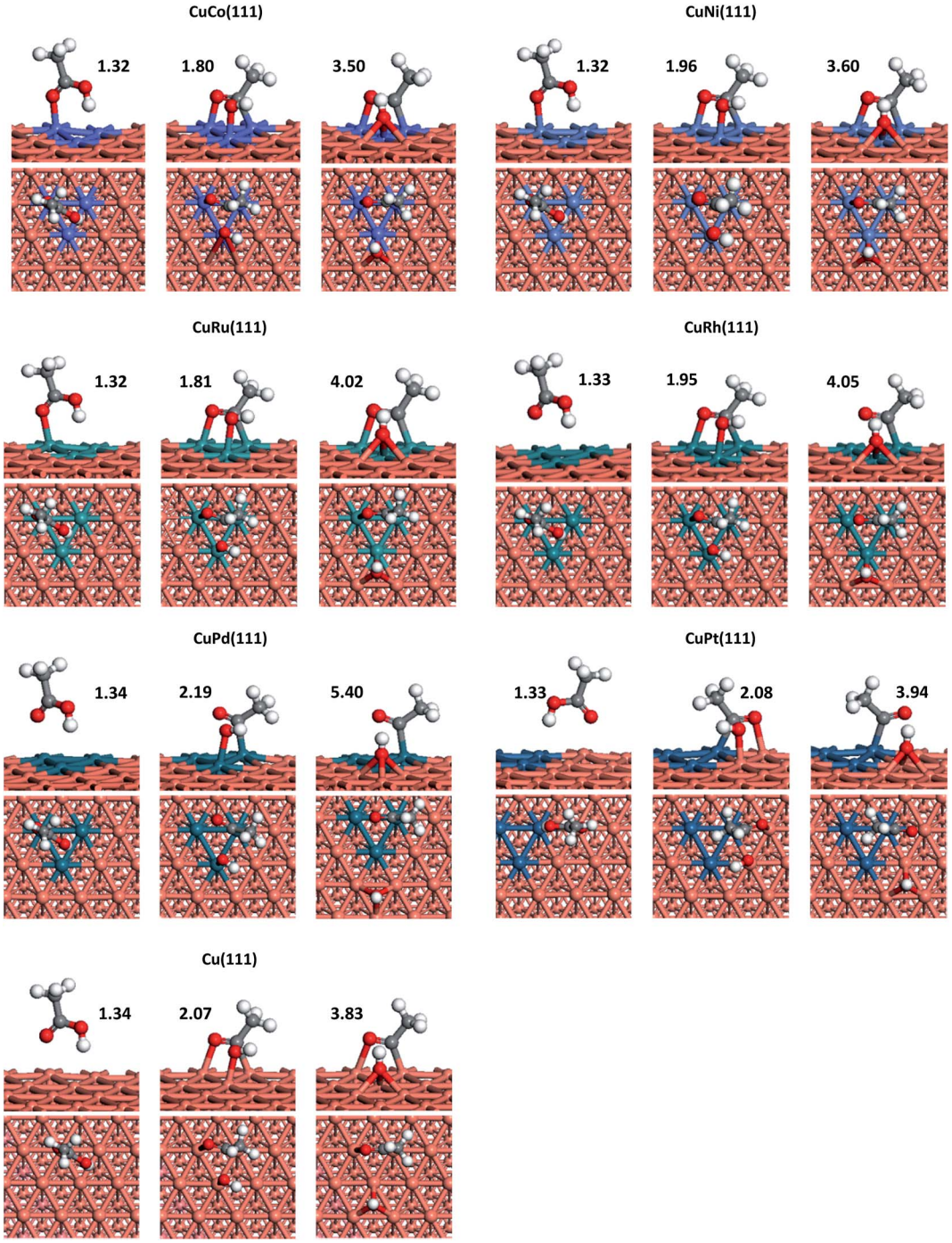

Fig. 1 Optimized configurations of the initial states (IS, left), transition states (TS, central) and final states (FS, right) for $CH_3COOH \rightarrow CH_3CO + OH$ reaction on Cu(111) and six doped-metal Cu(111) surfaces. C, O, H, and Cu atoms are shown in grey, red, white and orange balls, respectively. The length of C–OH is labelled and given in Å.

adsorption energies (listed in Table 2) on Cu(111) and six metal-doped Cu(111) surfaces and correlate these with the ability of activating C–OH bond of acetic acid.

As can be seen from Table 2, metals with higher C adsorption energies usually possess higher O adsorption energies in general (except Cu(111) surface). In the meanwhile, we find that the ability of C–OH scission appears to have a strong linear relationship with C adsorption energy (shown in Fig. 2a). However, O adsorption energy seems to be weaker dependent on activation barrier, indicating that the O adsorption energy has a secondary effect (Fig. 2b). Therefore, those metals with higher C (O adsorption energies in most cases) adsorption energies show better activity than metals with weaker ones. The reason is that stronger C adsorption can significantly improve C–metal interaction, which can weaken C–OH bond. Similarly, the metals which have stronger O adsorption energy can also

Table 1 Adsorption energies of acetic acid and reaction barriers of C–OH bond scission for acetic acid on Cu(111) and six doped-metal Cu(111) surfaces. All energy values are in eV

	Adsorption energy	$CH_3COOH \rightarrow CH_3CO + OH$	
Surface	(CH_3COOH)	Reaction barrier (E_a)	Reaction energy (ΔE)
CuCo(111)	0.84	0.14	−0.38
CuNi(111)	0.47	0.55	0.08
CuRu(111)	0.75	0.66	−0.09
CuRh(111)	0.46	0.74	0.24
CuPd(111)	0.32	1.47	0.74
CuPt(111)	0.37	1.23	0.59
Cu(111)	0.30	1.53	0.92

Table 2 Atomic adsorption energies of carbon and oxygen on Cu(111) and six doped-metal Cu(111) surfaces

	Adsorption energy (eV)						
Atom	CuCo	CuNi	CuRu	CuRh	CuPd	CuPt	Cu
O	6.57	5.88	5.60	5.02	3.99	3.81	4.81
C	7.60	6.92	7.06	6.82	5.34	5.72	4.88

prompt O–metal bond formation to some extent. Besides, as shown in Fig. 1, the products of C–OH bond scission of CH_3COOH are CH_3CO and OH, and CH_3CO prefer to adsorb on metal surfaces *via* both C and O(C=O) atoms, while OH favours to adsorb on metal surfaces with O atom. Therefore, on metals with higher C and even O adsorption energies, the co-adsorption of the terminal CH_3CO and OH species is more stable and thus the reverse action is less likely to occur. From another perspective, the strong C–metal interactions on these metal surfaces can withdraw electrons from C–OH bond and result in weakened C–OH bond. Herewith, it is not surprising that Co Ni, Ru, and even Rh with stronger C–metal and also O–metal interactions can enhance C–OH bond scission to varying degrees.

3.1.4 Brønsted–Evans–Polanyi (BEP) correlation for C–OH scission. Brønsted–Evans–Polanyi (BEP) correlations can be seen as predictive tools for estimating reaction barrier and two types of BEP correlations are usually described and applied in literatures.[6,26,51–58] One is correlating the activation barriers with the reaction energies for a single species on different metal surfaces (species-level BEP correlations). The other one is correlating the activation barriers with the reaction energies for a particular bond among multiple species across a serious of metal surfaces ("universal" BEP correlations).

In this section, the species-level BEP correlation is established to describe the relation between reaction energies and activation barriers for C–OH bond scission reactions on pure Cu and transition metal-doped Cu surfaces. As presented in Fig. 3, it is clear that there is a good linear relationship for C–OH bond cracking reactions of acetic acid on pure Cu and six metal-doped Cu surfaces. The correlation line whose fitted parameter is $R^2 = 0.951$ and slope is 1.079, is displayed in Fig. 3. Given that C–OH bond dissociation is an indispensable step for ethanol formation from acetic acid, current BEP correlation can be applied easily and directly to estimate the reaction barriers on other metal-doped Cu surfaces for C–OH bond scission of acetic acid when the adsorption configurations of reactants and products are similar qualitatively. It is so meaningful to examine a wide range of metals by only calculating adsorption energies of CH_3COOH and co-adsorption energies of CH_3CO and OH without determining transition states.

3.2 O–H bond formation of C_2-oxygenates

3.2.1 CH_3CHO adsorption. CH_3CHO is proved to be one of the main by-products over Cu-based catalysts in some experimental studies.[20–23,25,59] Similar conclusion could be obtained from our calculation results. The adsorption energy of CH_3CHO (0.22 eV) over Cu(111) is comparatively low, which means CH_3CHO adsorption on pure Cu surface is not very stable,

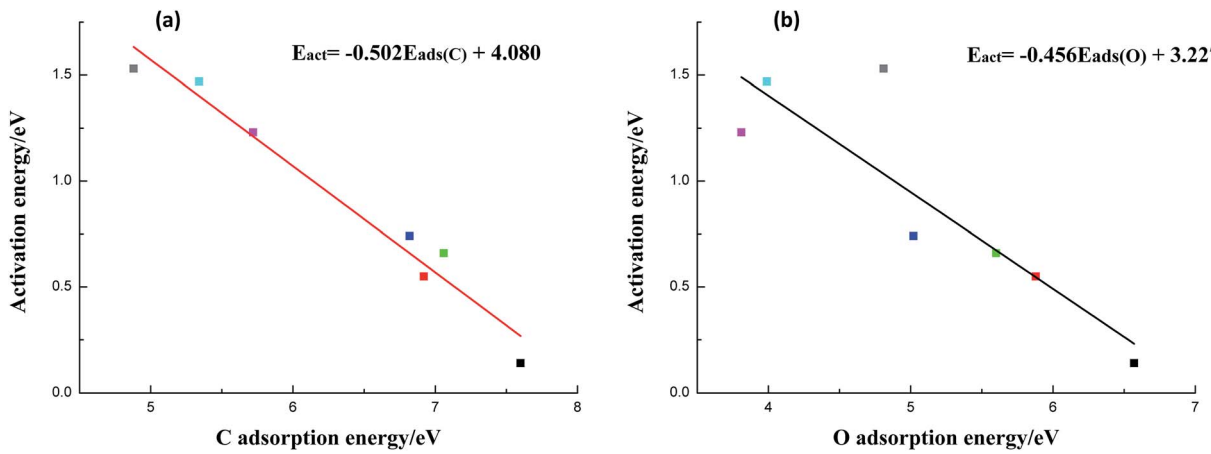

Fig. 2 Correlations between reaction barriers for the $CH_3COOH \rightarrow CH_3CO + OH$ reaction and: (a) adsorption energies of atomic C, (b) adsorption energies of atomic O on Cu(111) and six metal-doped Cu(111) surfaces (black: CuCo(111), red: CuNi(111), green: CuRu(111), dark blue: CuRh(111), pink: CuPt(111), light blue: CuPd(111) and grey: Cu(111)).

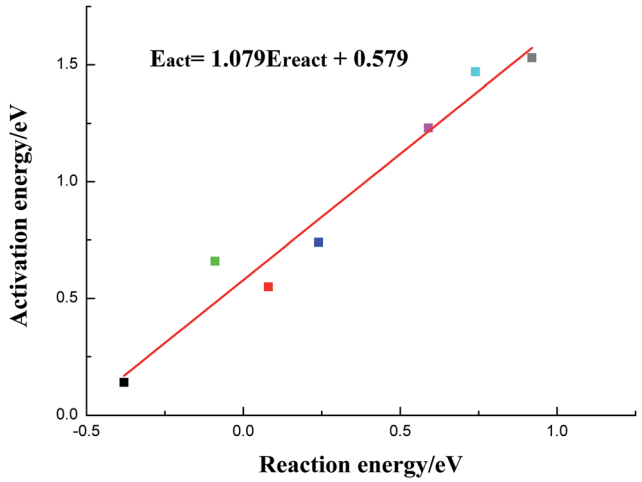

Fig. 3 Brønsted–Evans–Polanyi correlation for C–OH scission reaction of acetic acid on Cu(111) and six metal-doped Cu(111) surfaces (black: CuCo(111), red: CuNi(111), green: CuRu(111), dark blue: CuRh(111), pink: CuPt(111), light blue: CuPd(111) and grey: Cu(111)).

resulting in easy desorption of acetaldehyde as a side product. As a result, less CH_3CHO species might participate in the following hydrogenation reactions. It might be conducive to increase ethanol selectivity if the doped metals can strengthen CH_3CHO adsorption.

The most stable adsorption configurations and adsorption energies of CH_3CHO on pure Cu and doped-metal Cu surfaces are shown in Fig. 4 and Table 3. CH_3CHO binds to CuNi(111) surface in the bidentate configuration with O atom residing on top of one Ni atom and H atom residing on top site of neighbouring Ni atom. Likewise, the same case could be adopted on other metal-doped surfaces except on CuPt(111). The CH_3CHO adsorption energies on CuNi, CuCo, CuRu, CuRh and CuPd surfaces are 0.36, 0.71, 0.58, 0.36 and 0.21 eV, respectively. In contrast, CH_3CHO is preferentially adsorb on CuPt(111) *via* O atom near Cu top site and H atom on the adjacent Pt atom with adsorption energy 0.20 eV.

Similar to CH_3COOH adsorption, compared with the pure Cu(111) surface, doping of Co and Ru could greatly enhance CH_3CHO adsorption. Rh, Ni also show a minor contribution, while Pd and Pt have no positive effects on that.

3.2.2 O–H bond formation of C_2 oxygenates. O–H bond formation of C_2-oxygenates is an inevitable step for ethanol synthesis. However, related studies[14,17,51] indicated that C–H bond formation is more likely to take place than O–H bond formation during hydrogenation of C_1- or C_2-oxygenates. The C_2-oxygenates involved in ethanol synthesis are mainly CH_3CO, CH_3CHO and CH_3CH_2O. Reducing the reaction barriers of CH_3CO, CH_3CHO, CH_3CH_2O hydrogenation is a crucial route to increase the ethanol selectivity. Therefore, O–H bond formation of C_2-oxygenates, involving $CH_3CO + H \rightarrow CH_3COH$, $CH_3CHO + H \rightarrow CH_3CHOH$, $CH_3CH_2O + H \rightarrow CH_3CH_2OH$ on all these surfaces are examined. The other hydrogenation reactions on α-C atom of C_2-oxygenates are not considered here.

$CH_3CO + H \rightarrow CH_3COH$. As described above, CH_3CHO can easily desorb from Cu surface and serves as a by-product. However, compared with CH_3COH, CH_3CHO is more likely to

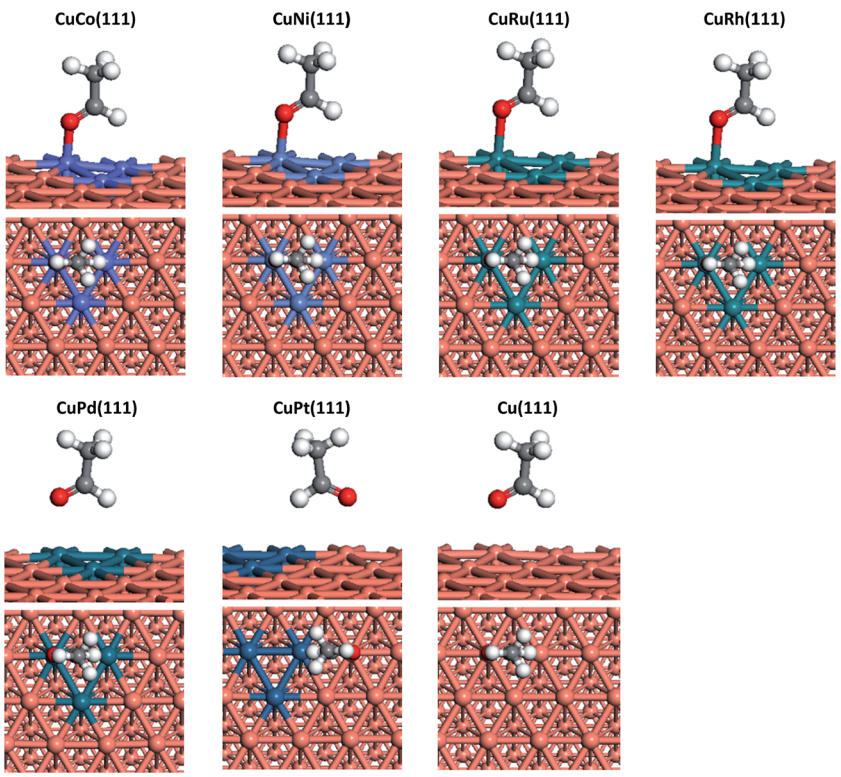

Fig. 4 Optimized adsorption configurations of CH_3CHO on Cu(111) and six doped-metal Cu(111) surfaces.

Table 3 Adsorption energies of C_2-oxygenates on Cu(111) and six metal-doped Cu(111) surfaces

	Adsorption energy (eV)		
Surface	CH_3CO	CH_3CHO	CH_3CH_2O
CuCo(111)	2.92	0.71	3.37
CuNi(111)	2.32	0.36	2.87
CuRu(111)	2.69	0.58	2.64
CuRh(111)	2.37	0.36	2.27
CuPd(111)	1.69	0.21	1.78
CuPt(111)	1.91	0.20	1.27
Cu(111)	1.37	0.22	2.30

generate from CH_3CO hydrogenation because of its low barrier as identified by others.[15] Therefore, if CH_3COH species formation from CH_3CO can be promoted, ethanol selectivity can be facilitated.

The most stable adsorption on pure Cu and all doped-metal Cu surfaces is tested, and the adsorption energies of CH_3CO are listed in Table 3. Similar to Cu(111), CH_3CO prefer to adsorb on the CuNi(111), CuCo(111), CuRu(111), CuRh(111), CuPd(111) surfaces *via* O atom on top site of doped metals and α-C atom at neighbouring top site. While on CuPt(111), O atom more likely to adsorb on top site of Cu atom rather than Pt atom. The reaction barriers for CH_3CO hydrogenation to CH_3COH on Ni-, Co-, Ru-, Rh-, Pd- and Pt-doped surfaces are 1.09, 1.09, 0.62, 0.76, 0.81 and 0.90 eV, respectively. Nevertheless, comparing with that on pure Cu surface (0.73 eV), only Ru can improve O–H bond formation. Other metals have no promotion effect (Pd and Rh) or even inhibit this elementary step (Pt, Ni and Co).

$CH_3CHO + H \rightarrow CH_3CHOH$. We examined the reaction barriers of CH_3CHOH formation from CH_3CHO on Cu(111) and six metal-doped Cu(111) surfaces as displayed in Table 4. The reaction barriers are 0.65 eV for CuNi(111), 0.85 eV for CuCo(111), 0.82 eV for CuRu(111), 0.52 eV for CuRh(111), 0.50 eV for CuPd(111) and 0.45 eV for CuPt(111), respectively. From these data, we can conclude the trend that less-oxophilic metals (Pt and Pd) might have better performance on this elementary step.

$CH_3CH_2O + H \rightarrow CH_3CH_2OH$. CH_3CH_2O is an important intermediate on Cu catalyst in acetic acid hydrogenation process since the reaction barrier of CH_3CH_2O hydrogenation to CH_3CH_2OH is high (1.11 eV), and the ethoxy adsorption is relatively strong (2.30 eV for adsorption energy), which means CH_3CH_2O species can be accumulated on Cu surface, the adsorption energies of CH_3CH_2O and reaction barriers of CH_3CH_2O hydrogenation are calculated and the results are listed in Tables 3 and 4.

CH_3CH_2O preferentially adsorbs on metal-doped Cu surfaces through O binding to doped-metals on hollow sites with C–C axis almost parallel to the surface. The only exception is CuPt(111), on which CH_3CH_2O adsorb on bridge site between two Pt atoms *via* O atom. The reaction barriers of CH_3CH_2O hydrogenation to CH_3CH_2OH are 1.69 eV for CuCo(111), 1.46 eV for CuNi(111), 1.30 eV for CuRu(111), 1.10 eV for CuRh(111), 0.59 eV for CuPd(111) and 0.19 eV for CuPt(111) in such a descending order. Compared with that on pure Cu surface (1.11 eV), Co, Ni, Ru and Rh can lead to CH_3CH_2O species adsorb more stably on Cu surface *via* O, resulting in more difficult hydrogenation on O atom of ethoxy species. In contrast, less-oxyphilic metal-doped surfaces, such as Pd and Pt, can greatly enhance the ability of ethoxy hydrogenation (CuPt and CuPd also exhibit high exothermicity).

The key descriptors over transition metal-doped Cu(111) surfaces and Cu(111) surface are summarized in Fig. 5. It can be concluded that weak adsorbates CH_3COOH and CH_3CHO can be stabilized significantly by oxophilic metals, especially for the case of dopants of Co and Ru. Less-oxyphilic metals (like Pt and Pd) seems to have negative effects on adsorption of CH_3COOH and CH_3CHO, while Ni and Rh have a certain promoting effect.

CH_3COOH disassociation to CH_3CO and OH is the most indispensable reaction on Cu catalyst since it might considerably influence ethanol productivity. The dopants of Co, Ni, Ru and Rh into Cu surface can activate C–OH bond of acetic acid greatly, and the most oxophilic metal Co shows the highest activity.

As for C_2-oxygenates hydrogenation reactions (O–H bond formation), in a general way, those metals with stronger oxophilicity are more likely to strengthen oxygenates *via* O atom, resulting in more difficult formation of O–H bond for C_2-oxygenates. However, the addition of less-oxophilic metals (Pt, Pd and even Rh) might lower the reaction barriers of O–H bond formation.

Therefore, optimum catalytic activity of Cu-based catalysts can be projected to be achieved on those metals which are capable of preferentially activating C–OH bond without

Table 4 The reaction barriers and reaction energies for O–H bond formation of C_2-oxygenates (acetyl, acetaldehyde and ethoxy) on Cu(111) and six metal-doped Cu(111) surfaces. All energy values are in eV

	$CH_3CO + H \rightarrow CH_3COH$		$CH_3CHO + H \rightarrow CH_3CHOH$		$CH_3CH_2O + H \rightarrow CH_3CH_2OH$	
Surfaces	Reaction barrier (E_a)	Reaction energy (ΔE)	Reaction barrier (E_a)	Reaction energy (ΔE)	Reaction barrier (E_a)	Reaction energy (ΔE)
CuCo(111)	1.09	0.79	0.85	0.19	1.69	1.21
CuNi(111)	1.09	0.55	0.65	0.17	1.46	0.92
CuRu(111)	0.62	0.24	0.82	0.27	1.30	0.60
CuRh(111)	0.76	0.19	0.52	0.03	1.10	0.22
CuPd(111)	0.81	0.44	0.50	0.10	0.59	−0.35
CuPt(111)	0.90	0.28	0.45	0.01	0.19	−0.80
Cu(111)	0.73	0.41	0.93	−0.08	1.11	0.13

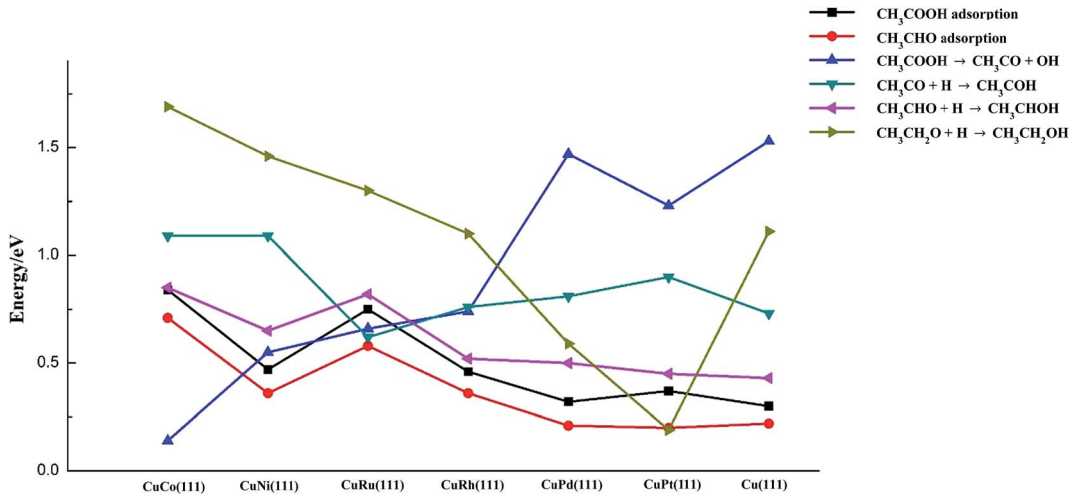

Fig. 5 The key descriptors for acetic acid hydrogenation to ethanol on Cu(111) and six metal-doped Cu(111) surfaces.

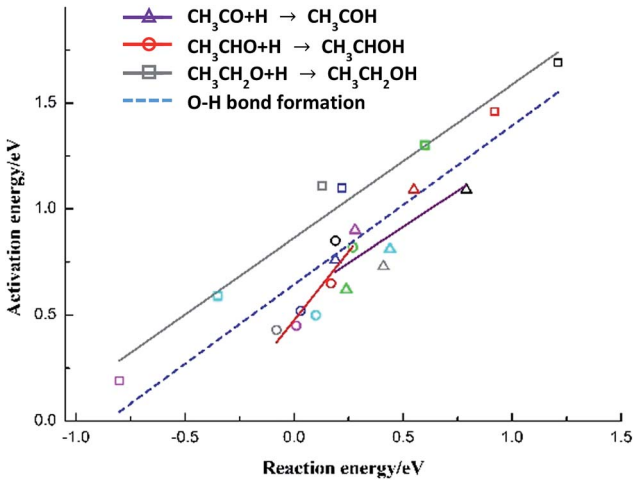

Fig. 6 Brønsted–Evans–Polanyi correlations for O–H bond formation reactions of C_2-oxygenates on Cu(111) and six metal-doped Cu(111) surfaces (black: CuCo(111), red: CuNi(111), green: CuRu(111), dark blue: CuRh(111), pink: CuPt(111), light blue: CuPd(111) and gray: Cu(111)).

Table 5 The fitted parameters of Brønsted–Evans–Polanyi correlations for O–H bond formation reactions

Reaction	Slope (eV)	Intercept (eV)	R^2
$CH_3CO + H \rightarrow CH_3COH$	0.678 ± 0.241	0.575 ± 0.110	0.537
$CH_3CHO + H \rightarrow CH_3CHOH$	1.296 ± 0.281	0.475 ± 0.041	0.771
$CH_3CH_2O + H \rightarrow CH_3CH_2OH$	0.723 ± 0.056	0.864 ± 0.039	0.966
O–H formation of C_2-oxygenates	0.749 ± 0.097	0.644 ± 0.048	0.744

considerably inhibiting O–H bond formation of C_2-oxygenates. We can see from Fig. 5 that CuCo and CuNi have more activity for C–OH bond cracking, while for O–H bond formation reactions of C_2-oxygenates, the barriers on these metals are relatively high, even higher than those on pure Cu surface. In contrast, C_2-oxygenates hydrogenation reactions are more likely to occur on CuPd and CuPt, but C–OH cleave ability is so fragile on these surfaces. Therefore, it seems like CuRh and CuRu possess moderate C–OH bond scission barriers and three C_2-oxygenates hydrogenation barriers, which means CuRh and CuRu are likely to possess better performance for ethanol synthesis from acetic acid hydrogenation (between these two metals, CuRh has slightly lower barriers for O–H bond formation reactions, while CuRu has stronger adsorption for acetic acid and acetaldehyde as well as lower C–OH bond breaking barrier). Olcay *et al.*[10] reported findings of experimental study on the aqueous-phase hydrogenation of acetic acid catalyzed by transition metals such as Ru, Rh, Pd, Ni, Cu, Ir, and Pt, and the result indicated that Ru and Rh exhibit better performance for acetic acid hydrogenation to ethanol compared to other metals. Their result might be a support for our conclusion in a certain degree.

The species-level BEP correlations for each C_2-oxygenate (CH_3CO, CH_3CHO and CH_3CH_2OH) hydrogenation reaction are also developed, as presented in Fig. 6 with corresponding parameters listed in Table 5. More than that, all the points for three hydrogenations reactions of C_2-oxygenates on Cu(111) and metal-doped Cu(111) surfaces are regressed together to develop an all-metal BEP relationship for O–H bond formation ("universal" BEP correlation for O–H). The slope is 0.749 with intercept 0.644 and R^2 0.744, which indicates that O–H formation steps of C_2-oxygenates show a tendency to have the mid-to-late transition states.[6,53] Similarly, these correlations can also be used to achieve more insights into the chemical trends of these elementary steps on a series of metals, and meanwhile, it can provide a reference for further studies and can be consummated with regressing more calculation data.

4. Conclusions

In the present work, in order to investigate the effects of transition metal dopants on the catalytic activity of Cu(111) surface toward ethanol synthesis *via* acetic acid hydrogenation, the adsorption of key species and key elementary reactions on pure

Cu and six metal-doped Cu surfaces were calculated using density functional theory. The performance of different doped transition metals for C–OH bond scission of acetic acid was systematically investigated. The results indicated that oxophilic metals, such as Co, Ni, Ru, are projected to greatly enhance acetic acid adsorption and C–OH bond scission. The activation energies for C–OH cracking reactions generally decline with increasing C adsorption energies, while O adsorption energy shows a second effect, which means the cleavage of C–OH bond in acetic acid is more facile on oxophilic metal-doped surfaces (especially Co, Ru and Ni). The BEP correlation for C–OH cracking reaction on all metal-doped Cu surfaces showed a good relation between activation energies and reaction energies. It is meaningful for us to test the activity of other Cu–metal surfaces only with adsorption energy calculations of reactants and products. CH_3CHO adsorption and the reaction barriers of O–H bond formation of C_2-oxygenates are also examined. Metals with more oxophilicity (Co and Ni) could enhance CH_3CHO adsorption but inhibit O–H bond formation.

In conclusion, those metal-doped Cu-based catalysts which are capable of preferentially activating C–OH bond without considerably inhibiting O–H bond formation of C_2-oxygenates, are predicted to achieve optimum catalytic activity for ethanol formation from acetic acid hydrogenation (like Ru and Rh). This work can provide helpful and theoretical guidance for experimental studies and designing of proper Cu-based catalysts for acetic acid hydrogenation to ethanol.

Acknowledgements

This work was supported by the National Natural Science Foundation of China (No. 21406159).

References

1 H. N. Chang, N. Kim, J. Kang and C. M. Jeong, *Biotechnol. Bioprocess Eng.*, 2010, **15**, 1–10.
2 W. Chen, Y. Ding, D. Jiang, T. Wang and H. Luo, *Catal. Commun.*, 2006, **7**, 559–562.
3 B. Q. Xu and W. Sachtler, *J. Catal.*, 1998, **180**, 194–206.
4 N. Bion, D. Duprez and F. Epron, *ChemSusChem*, 2012, **5**, 76–84.
5 A. Bshish, Z. Yaakob, B. Narayanan, R. Ramakrishnan and A. Ebshish, *Chem. Pap.*, 2011, **65**, 251–266.
6 J. E. Sutton and D. G. Vlachos, *Ind. Eng. Chem. Res.*, 2015, **54**, 4213–4225.
7 W. Rachmady and M. A. Vannice, *J. Catal.*, 2000, **192**, 322–334.
8 R. Alcala, J. W. Shabaker, G. W. Huber, M. A. Sanchez-Castillo and J. A. Dumesic, *J. Phys. Chem. B*, 2005, **109**, 2074–2085.
9 V. Pallassana and M. Neurock, *J. Catal.*, 2002, **209**, 289–305.
10 H. Olcay, L. Xu, Y. Xu and G. W. Huber, *ChemCatChem*, 2010, **2**, 1420–1424.
11 H. Olcay, Y. Xu and G. W. Huber, *Green Chem.*, 2014, **16**, 911–924.
12 X. Sun, R. Zhang and B. Wang, *Appl. Surf. Sci.*, 2013, **265**, 720–730.
13 J. Wang, X. Zhang, Q. Sun, S. Chan and H. Su, *Catal. Commun.*, 2015, **61**, 57–61.
14 X. Xu, J. Su, P. Tian, D. Fu, W. Dai, W. Mao, W. Yuan, J. Xu and Y. Han, *J. Phys. Chem. C*, 2015, **119**, 216–227.
15 H. Zheng, R. Zhang, Z. Li and B. Wang, *J. Mol. Catal. A: Chem.*, 2015, **404–405**, 115–130.
16 L. C. Grabow and M. Mavrikakis, *ACS Catal.*, 2011, **1**, 365–384.
17 J. Wang, Y. Kawazoe, Q. Sun, S. Chan and H. Su, *Surf. Sci.*, 2016, **645**, 30–40.
18 Y. Yang, M. G. White and P. Liu, *J. Phys. Chem. C*, 2012, **116**, 248–256.
19 R. Zhang, G. Wang and B. Wang, *J. Catal.*, 2013, **305**, 238–255.
20 S. Harnos, G. Onyestyák and J. Valyon, *Appl. Catal., A*, 2012, **439–440**, 31–40.
21 G. Onyestyák, S. Harnos and D. Kalló, *Catal. Commun.*, 2012, **26**, 19–24.
22 S. Harnos, G. Onyestyák and D. Kalló, *Microporous Mesoporous Mater.*, 2013, **167**, 109–116.
23 G. Onyestyák, S. Harnos, M. Štolcová, A. Kaszonyi and D. Kalló, *Catal. Commun.*, 2013, **40**, 32–36.
24 G. Onyestyák, S. Harnos, C. Badari, E. Drotár, S. Klébert and D. Kalló, *Open Chem.*, 2015, **13**, 517–527.
25 G. Onyestyák, S. Harnos, S. Klébert, M. Štolcová, A. Kaszonyi and D. Kalló, *Appl. Catal., A*, 2013, **464–465**, 313–321.
26 P. Ferrin, D. Simonetti, S. Kandoi, E. Kunkes, J. A. Dumesic, J. K. Nørskov and M. Mavrikakis, *J. Am. Chem. Soc.*, 2009, **131**, 5809–5815.
27 N. D. Subramanian, G. Balaji, C. S. S. R. Kumar and J. J. Spivey, *Catal. Today*, 2009, **147**, 100–106.
28 N. Schumacher, K. Andersson, L. C. Grabow, M. Mavrikakis, J. Nerlov and I. Chorkendorff, *Surf. Sci.*, 2008, **602**, 702–711.
29 G. Prieto, S. Beijer, M. L. Smith, M. He, Y. Au, Z. Wang, D. A. Bruce, K. P. de Jong, J. J. Spivey and P. E. de Jongh, *Angew. Chem., Int. Ed.*, 2014, **53**, 6397–6401.
30 Y. Zhao, K. Sun, X. Ma, J. Liu, D. Sun, H. Su and W. Li, *Angew. Chem., Int. Ed.*, 2011, **50**, 5335–5338.
31 M. Behrens, F. Studt, I. Kasatkin, S. Kuehl, M. Haevecker, F. Abild-Pedersen, S. Zander, F. Girgsdies, P. Kurr, B. Kniep, M. Tovar, R. W. Fischer, J. K. Nørskov and R. Schloegl, *Science*, 2012, **336**, 893–897.
32 F. Studt, F. Abild-Pedersen, Q. Wu, A. D. Jensen, B. Temel, J. Grunwaldt and J. K. Nørskov, *J. Catal.*, 2012, **293**, 51–60.
33 J. Liu, H. Su, D. Sun, B. Zhang and W. Li, *J. Am. Chem. Soc.*, 2013, **135**, 16284–16287.
34 G. Li, Q. Wang, D. Li, X. Lue and J. He, *Phys. Lett. A*, 2008, **372**, 6764–6769.
35 Y. Zhao, M. Yang, D. Sun, H. Su, K. Sun, X. Ma, X. Bao and W. Li, *J. Phys. Chem. C*, 2011, **115**, 18247–18256.
36 V. Glezakou, J. E. Jaffe, R. Rousseau, D. Mei, S. M. Kathmann, K. O. Albrecht, M. J. Gray and M. A. Gerber, *Top. Catal.*, 2012, **55**, 595–600.
37 W. Luo and A. Asthagiri, *J. Phys. Chem. C*, 2014, **118**, 15274–15285.

38 R. Zhang, G. Wang, B. Wang and L. Ling, *J. Phys. Chem. C*, 2014, **118**, 5243–5254.
39 R. A. van Santen, M. Ghouri and E. M. J. Hensen, *Phys. Chem. Chem. Phys.*, 2014, **16**, 10041–10058.
40 A. J. Medford, A. C. Lausche, F. Abild-Pedersen, B. Temel, N. C. Schjodt, J. K. Norskov and F. Studt, *Top. Catal.*, 2014, **57**, 135–142.
41 A. N. Pour, Z. Keyvanloo, M. Izadyar and S. M. Modaresi, *Int. J. Hydrogen Energy*, 2015, **40**, 7064–7071.
42 Y. K. Zhang and W. T. Yang, *Phys. Rev. Lett.*, 1998, **80**, 890.
43 M. Ernzerhof, J. P. Perdew, K. Burke and M. Ernzerhof, *Phys. Rev. Lett.*, 1998, **80**, 891.
44 B. Hammer and J. K. Nørskov, *Adv. Catal.*, 2000, **45**, 71–129.
45 Q. Fu and Y. Luo, *J. Phys. Chem. C*, 2013, **117**, 14618–14624.
46 J. Greeley and M. Mavrikakis, *Nat. Mater.*, 2004, **3**, 810–815.
47 J. Nerlov, S. Sckerl, J. Wambach and I. Chorkendorff, *Appl. Catal., A*, 2000, **191**, 97–109.
48 B. Delley, *J. Phys. Chem. C*, 1990, **92**, 508.
49 B. Delley, *J. Phys. Chem. C*, 2000, **113**, 7756.
50 J. L. C. Fajín, M. N. D. S. Cordeiro, F. Illas and J. R. B. Gomes, *J. Catal.*, 2014, **313**, 24–33.
51 J. E. Sutton and D. G. Vlachos, *ACS Catal.*, 2012, **2**, 1624–1634.
52 S. Wang, V. Vorotnikov, J. E. Sutton and D. G. Vlachos, *ACS Catal.*, 2014, **4**, 604–612.
53 E. D. German and M. Sheintuch, *J. Electroanal. Chem.*, 2011, **660**, 261–275.
54 S. Wang, B. Temel, J. Shen, G. Jones, L. C. Grabow, F. Studt, T. Bligaard, F. Abild-Pedersen, C. H. Christensen and J. K. Nørskov, *Catal. Lett.*, 2011, **141**, 370–373.
55 J. Cheng, P. Hu, P. Ellis, S. French, G. Kelly and C. M. Lok, *J. Phys. Chem. C*, 2008, **112**, 1308–1311.
56 R. A. V. Santen, M. Neurock and S. G. Shetty, *Chem. Rev.*, 2010, **110**, 2005–2048.
57 D. Loffreda, F. Delbecq, F. Vigné and P. Sautet, *Angew. Chem., Int. Ed.*, 2009, **48**, 8978–8980.
58 T. Bligaard, J. K. Nørskov, S. Dahl, J. Matthiesen, C. H. Christensen and J. Sehested, *J. Catal.*, 2004, **224**, 206–217.
59 M. A. N. Santiago, M. A. Sánchez-Castillo, R. D. Cortright and J. A. Dumesic, *J. Catal.*, 2000, **193**, 16–28.